

# Graphene Oxide/Vinyl Ester Resin Nanocomposite: Effect of Graphene Oxide, Thermal Stability, and Modeling of the Curing Kinetics

V. Arabli\* and A. Aghili\*\*

\*National Iranian Oil Company, Supervision on Petroleum Export  
Tehran 15936, Iran, arably@yahoo.com

\*\*Department of Polymer Engineering, Shiraz Branch  
Islamic Azad University, Shiraz, Iran, aghili@iaushiraz.ac.ir

## ABSTRACT

Graphene oxide (GO) was synthesized and nanocomposites were prepared using different contents of the GO and vinyl ester resin (VE). The nonisothermal differential scanning calorimetry (DSC) was used to study the cure kinetics of VE and 0.3wt% GO/VE nanocomposite. Kissinger and Ozawa equations were used to determine the activation energy ( $E_a$ ). The  $E_a$  values of the cured GO/VE nanocomposite showed a decrease with respect to the neat VE. It is concluded that GO has a catalytic effect in the cure reaction. The dynamic curing process was modeled to predict the degree of curing and curing rate of resin. Scanning electron microscopy (SEM) was studied to discern the surface features and dispersion of GO. The thermal stability of the cured VE and its nanocomposite was investigated with thermogravimetric analysis (TGA).

**Keywords:** Graphene Oxide; Epoxy Vinyl Ester Resin; Cure Kinetics; Modeling; Thermal Stability.

## 1 INTRODUCTION

Vinyl ester resins are thermoset matrices that are widely used in the composites industry [1]. VE resin is produced by the esterification of epoxy resin with unsaturated monocarboxylic acid. The resins are widely used in environments that require high corrosion and chemical resistance, water barrier properties, low moisture absorption, low shrinkage and good dimensional stability [2]. Generally, these resins have been used in a range of applications as a matrix material, coating, wide adhesive, electronic encapsulant, in the marine industry, pipelines and automobiles [3]. The thermoset epoxy polymers can be mixed with a second phase of nanofillers such as nanospheres, nanotubes, nanoplatelets, etc. These nanocomposites improve the toughness, stiffness, strength and thermal properties. As a layered carbon nanomaterial, graphene with high aspect ratios is widely used to improve mechanical, thermal and electrical properties in polymer materials. However, the high cost and poor dispersion of the CNTs and CNFs in the polymers, limits the range of practical application [4].

## 2 EXPERIMENTAL

### 2.1 Materials

Natural graphite flakes (100 meshes) were supplied by Sigma-Aldrich (Saint Louis, USA). Farapol V301 epoxy vinyl ester resin using bisphenol A epoxy (42 wt% styrene content) was purchased from Farapol (Hamadan, Iran). Cobalt, dimethylaniline (DMA) and methyl ethyl ketone peroxide (MEKP), sulfuric acid ( $H_2SO_4$ ), phosphoric acid ( $H_3PO_4$ ), potassium permanganate ( $KMnO_4$ ), hydrogen peroxide ( $H_2O_2$ ), hydrochloric acid (HCl), tetrahydrofuran (THF) solvent and other chemicals were purchased from Merck Chemicals Company.

### 2.2 Devices and Equipment

DSC and TGA were measured by a Mettler Toledo. SEM images were taken by a TESCAN Vega TS 5136mm. XRD was measured using a Bruker D/Max2550 V X-ray diffractor. A UP400S sonicator (Hielscher, DE) was used for dispersion of graphene oxide in the GO/VE nanocomposite.

### 2.3 Synthesis and Preparation of GO

The improved method of Hummers [5] was used to prepare GO from graphite flakes. For this purpose, a mixture of concentrated  $H_2SO_4/H_3PO_4$  (360 : 40 mL) was added gradually with stirring to a mixture of graphite flakes/ $KMnO_4$  (3 : 18 g). Then, the reaction was warm up to 45 °C and mixed for 12 h. The reaction was cooled and poured onto 400 g ice with 3mL of 30% hydrogen peroxide ( $H_2O_2$ ). The mixture was sifted through a metal sieve (Sigma-Aldrich, 300  $\mu m$ ) and then filtered by polyester fiber. The filtrate materials were centrifuged at 4000 rpm for 4 h, and solid product was separated. The solid product was then washed with 200 mL of water, 200 mL of 30% HCl, and 200 mL of ethanol, respectively. After each wash, the mixture was then purified following the previous protocol of sifting, filtering and centrifugation. The material remaining was coagulated with 200 mL of ether, and the mixture was filtered again. The resulting GO obtained on the filter was vacuum dried overnight at room temperature to produce the GO powder. The resulted GO was placed into a crucible, and the crucible was put into a furnace (preheated to 1050 °C for 30 s) to obtain the graphene.

## 2.4 Preparation of GO/VE Nanocomposite

Different weight contents of GO (0.1, 0.3, 1.5, 3.0 wt%) were first ultrasonicated in 50 mL of THF solvent for 1 h. The homogeneous solution of GO, in THF, was then mixed with 100 g VE monomer. The mixture stirred and ultrasonicated, for 30 min. The mixture was degassed at 60 °C in a vacuum oven for 10 h. Afterwards, 1.5 mL MEKP (catalyst) and 0.3% cobalt (accelerator) were added and the mixture stirred again. Then, the cured sample were pre-cured in an oven at 80°C for 2 h and post-cured at 120 °C for another 1 h.

## 2.5 DSC and TGA

25 mg of the uniform viscous mixture was put in the DSC sample cell at room temperature. The sample was heated by constant heating rate (5, 10 and 15 °C /min) from 25 to 160 °C under nitrogen gas flow of 22 ml/min. Degradation and weight loss of the VE and its nanocomposite was investigated by the TGA system under nitrogen gas flow of 22 ml/min and heating rate of 10 °C/min.

## 3 RESULTS AND DISCUSSION

### 3.1 XRD Evaluation

XRD patterns of graphite, graphene oxide and GO/VE nanocomposite are shown in Fig. 1. The peak at  $2\theta = 26.55$  for graphite corresponds to the diffraction of the (002) graphite plane composed to an interlayer spacing of 0.355 nm [6]. The peak at  $2\theta = 9.45$  (graphene oxide) corresponds to the diffraction of the (002) graphene oxide plane. The interlayer spacing of the graphene oxide can be obtained according to Bragg's law:  $n\lambda = 2d \sin \theta$

where  $n$  is the diffraction series,  $\lambda$  is the X-ray wavelength, and  $d$  is the interlayer spacing of graphene oxide. The calculated value of  $d$  (0.935 nm), implies that the sample is expanded when graphite is oxidized. However, this peak has disappeared in graphene, indicating that the distances between the graphene layers have been greatly expanded and the layers are disordered [7].

### 3.2 Curing Kinetics and Modeling

Non-isothermal (DSC) was used to study the kinetics of the cure reaction of VE and its nanocomposite. The results are shown in Fig. 2. The values of peak temperatures and heats of reaction are shown in Table 1. All kinetic models have a same basic equation:

$$\frac{d\alpha}{dt} = k(T)f(\alpha) \quad (1)$$

where  $da/dt$  is the cure reaction rate,  $k(T)$  is the rate constant,  $\alpha$  is the fractional conversion at a time  $t$ ,  $f(\alpha)$  is function of  $\alpha$ . A kinetic model for a dynamic curing process with a constant heating rate can be explained as [8]:

$$\frac{d\alpha}{dt} = Ae^{-Ea/RT} \alpha^m (1-\alpha)^n \quad (2)$$

where  $k(T)$  and  $f(\alpha)$  are replaced by Arrhenius equation and an equation based on an autocatalytic model, respectively.  $A$  is the pre-exponential factor,  $E_a$  is the activation energy,  $R$  is the gas constant, and  $T$  is the absolute temperature. The correlation between  $da/dt$  and  $da/dT$  can be explained:

$$\frac{d\alpha}{dt} = \left(\frac{dT}{dt}\right) \frac{d\alpha}{dT} \quad (3)$$

where  $dT/dt$  is constant heating rate. Substituting Eq. (2) and (3) gives:

$$\frac{d\alpha}{dT} = A \left(\frac{dT}{dt}\right)^{-1} \alpha^m (1-\alpha)^n \exp\left(\frac{-Ea}{RT}\right) \quad (4)$$

Following form is general linear eq. between the heating rate and peak temperature  $T_p$  as Ozawa [9] method:

$$\ln\left(\frac{dT}{dt}\right) = c + \left(\frac{-Ea}{R}\right)\left(\frac{1}{T}\right) \quad (5)$$

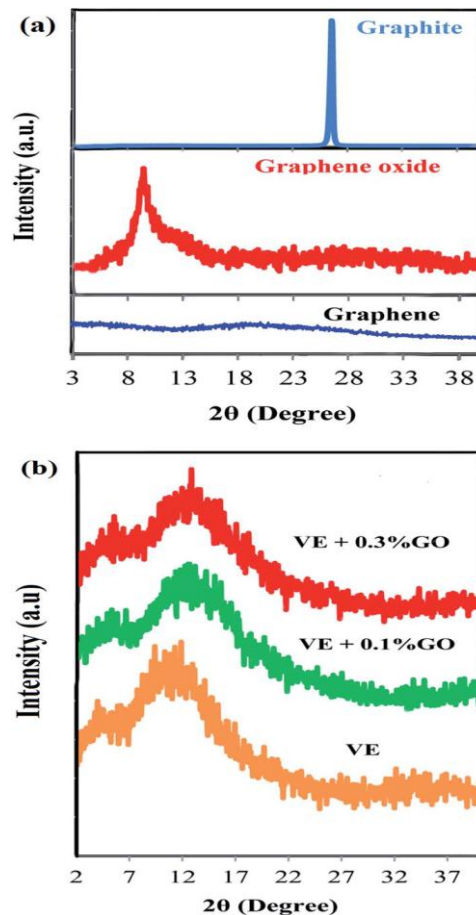


Fig. 1: XRD patterns of (a) graphite, graphene oxide, and graphene, (b) neat VE and its composites containing different contents of GO.

Sample	VE			VE + 0.3% GO		
$q$ ( $^{\circ}\text{C}/\text{min}$ )	5	10	15	5	10	15
$T_p$ (K)	350.15	363.65	372.55	351.15	366.45	374.25
Exo. Heat (J/g)	65.06	65.13	61.84	71.18	66.12	63.98

Table 1: Dynamic DSC data for the curing of resin at different heating rates.

Sample	VE	VE + 0.3% GO
$E_a^a$ (kJ/mol)	56.6	43.6
$E_a^b$ (kJ/mol)	59.8	49.0

<sup>a</sup> Kissinger method, <sup>b</sup> Ozawa method

Table 2:  $E_a$  values from Kissinger and Ozawa methods.

Equation (6) indicates Kissinger eq. [10].

$$-\ln\left(\frac{q}{T_p^2}\right) = \frac{E_a}{RT_p} - \ln\left(\frac{AR}{E_a}\right) \quad (6)$$

where  $q$  is the heating rate. A plot of  $\ln(q/T_p^2)$  versus  $1/T_p$  was made as a Kissinger plot and also  $\ln(q)$  versus  $1/T_p$  was made as an Ozawa plot for peaks of the individual DSC curves. Values of activation energies for each peak are shown in Table 2. By comparing the  $E_a$  for both systems of resin (VE and VE + 0.3% GO), it can be suggested that GO as a catalyst, improved the cure reaction and decreased  $E_a$  values. Having the activation energies ( $E_a$ ) for both reactions, a multiple nonlinear least-squares regression method based on the Levenberg–Marquardt algorithm [8] was used to find the best values for the system of ordinary

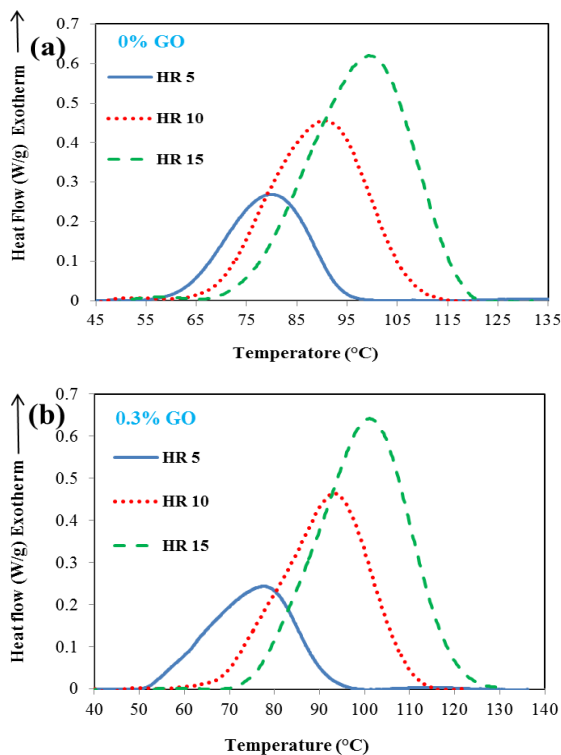


Figure 2: DSC curves (a) VE (b) VE + 0.3% GO.

pre-exponential factor ( $A$ ) and reaction orders ( $m$  and  $n$ ) for each reactions (peaks). These dynamic kinetic parameters are listed in Table 3 for all heating rates. Having obtained the kinetic parameters for reactions, we can calculate the values for degree of cure ( $\alpha$ ) and cure rate ( $d\alpha/dt$ ) for each reaction by solving the system of differential equations:

$$\frac{d\alpha}{dT} = \left(\frac{dT}{dt}\right)^{-1} A e^{-(E_a/RT)} \alpha^m (1-\alpha)^n \quad (7)$$

Differential equations has been solved using Matlab software. A program based on the Runge–Kutta (4, 5) algorithm was used to find the numerical solution for eq. (7). The calculated values of degree of cure ( $\alpha$ ) versus temperature and experimental results for VE + 0.3% GO at all heating rate, are shown in Fig. 3. The calculated degree of cure ( $\alpha$ ) agreed well with the experimental data for all heating rates. The cure rate  $d\alpha/dt$  versus temperature was obtained by using eq. (3). The predicted results and experimental data are shown in Fig. 4.

### 3.3 Scanning electron microscopy (SEM)

SEM test was used to study the different morphologies of the fracture surface (fig. 5). As shown in Fig. 5, the surface of neat VE is almost smooth. VE prepared with different amounts of GO show a rough fracture surface. It can be concluded that a rough surface can be attributed to the polymer deformation [11].

### 3.4 Thermal Stability

Fig. 6 shows the TGA curves of cured VE and its nanocomposite. It can be observed that the thermal degradation of nanocomposite takes place at higher temperatures than the neat resin. The char yields at  $593^{\circ}\text{C}$  increased from 6.8% to 15.2% with increasing GO contents to the VE. The increased thermal stability with addition of GO sheets is attributed to a higher heat capacity of the sheets and a better barrier effect of GO sheets. These effects retard the volatilization of polymer decomposition products. The increasing of char yields agrees with the mechanism of flame retardancy. Thus, the addition of GO improved the polymer thermal resistance and flame retardancy [12].

## 4 CONCLUSION

Effect of GO on the cure kinetics of VE in the presence of 0.3% wt GO was studied. To determine activation energy of the cure reaction of VE, non-isothermal DSC method, Ozawa and Kissinger equations were used. The  $E_a$  value of

cure reaction of VE in the presence of 0.3% GO decreased. It is concluded that GO acted as catalyst in the reaction of VE/GO. DSC curves were modeled by Matlab program. The char yields increased with the addition of GO to the resin and improved the polymer flame retardancy and thermal resistance at high temperatures.

Sample	Heating rate (°C/min)	$A_r$	$m$	$n$
VE	5	0.12583	0.53746	0.9475
	10	0.14729	0.50535	1.0254
	15	0.14210	0.48115	0.9262
VE+ 0.3% GO	5	0.12213	0.44666	0.8000
	10	0.12652	0.55969	0.8610
	15	0.14395	0.53159	0.9103

Table 3: Dynamic kinetic parameters obtained by a multiple nonlinear least-squares regression.

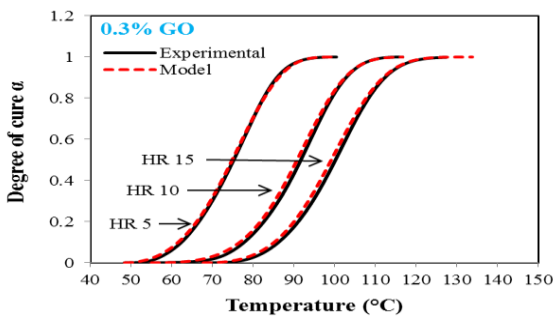


Figure 3: Comparison of model and experimental data for degree of cure as a function of temperature for VE + 0.3% GO at heating rate of 5, 10 and 15 °C/min.

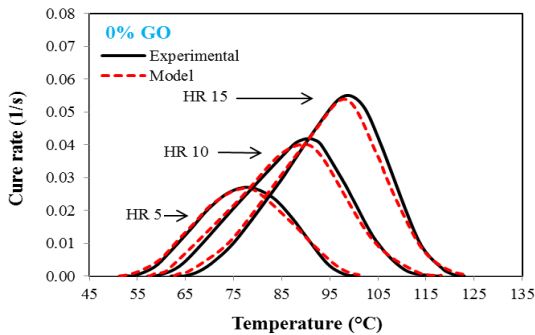


Figure 4: Comparison of model and experimental data for cure rate as a function of temperature for VE + 0.3% Go at heating rate of 5, 10 and 15 °C/min.

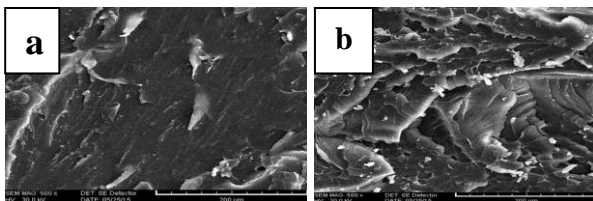


Figure 5: SEM image of fracture surfaces of VE and GO/VE nanocomposite, (a) neat VE, (b) 0.3 wt% of GO.

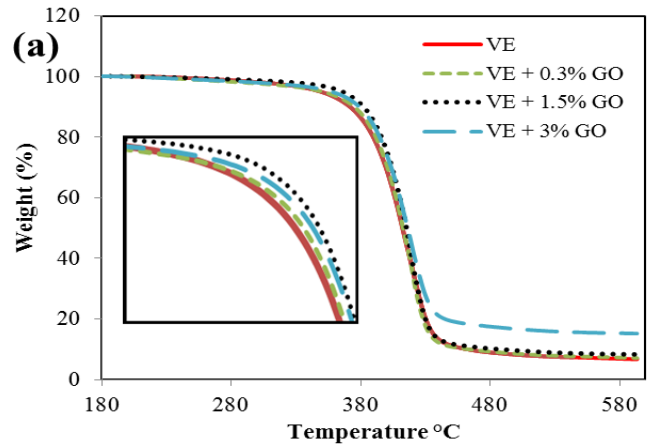


Figure 6: TGA curves of VE and its nanocomposite.

## ACKNOWLEDGEMENT

The authors would like to thank the National Iranian Oil Company research and technology directory for its financial support.

## REFERENCES

- [1] C. Jang, T. E. Lacy, S. R. Gwaltney, H. Toghiani and C. U. Pittman, *Macromolecules*, 45, 4876, 2012.
- [2] A. Chaturvedi and A. Tiwari, *Adv. Mater. Lett.*, 4, 656, 2013.
- [3] X. Zhang, V. Bitaraf, S. Wei and Z. Guo, *AIChE J.*, 60, 266, 2014.
- [4] Z. Wang, P. Wei, Y. Qian and J. Liu, *Composites, Part B*, 60, 341, 2014.
- [5] W. S. Hummers and R. E. Offeman, *J. Am. Chem. Soc.*, 80, 1339, 1958.
- [6] H.-K. Jeong, Y. P. Lee, R. J. W. E. Lahaye, M.-H. Park, K. H. An, I. J. Kim, C.-W. Yang, C. Y. Park, R. S. Ruoff and Y. H. Lee, *J. Am. Chem. Soc.*, 130, 1362, 2008.
- [7] D. A. Nguyen, Y. R. Lee, A. V. Raghu, H. M. Jeong, C. M. Shin and B. K. Kim, *Polym. Int.*, 58, 412, 2009.
- [8] L. Sun, S. S. Pang, A. M. Sterling, I. I. Negulescu, M. A. Stubblefield, *J. Appl. Polym. Sci.* 86, 1911, 2002.
- [9] T. J. Ozawa, *Therm. Anal.* 2, 301, 1970.
- [10] H. E. Kissinger, *Anal. Chem.* 29, 1702, 1957.
- [11] J. Zhu, S. Wei, J. Ryu, M. Budhathoki, G. Liang and Z. Guo, *J. Mater. Chem.*, 20, 4937, 2010.
- [12] Q. Liu, X. Zhou, X. Fan, C. Zhu, X. Yao and Zh. Liu, *Polym.- Plast. Technol. Eng.*, 51, 251, 2012.